# Applications of heavy-negative-ion sources for materials science (invited)

Junzo Ishikawa[a)]
*Department of Electronic Science and Engineering, Kyoto University, Sakyo-ku, Kyoto 606-8501, Japan*

(Presented on 8 September 1999)

Applications of heavy negative ions produced by sputter-type negative-ion sources for materials science are reviewed. Submilliampere and milliampere heavy-negative-ion beams can be produced by a neutral- and ionized-alkaline–metal-bombardment-type heavy-negative-ion source and rf plasma sputter-type negative-ion sources, respectively. These negative-ion beams can be applied for materials processing such as ion implantation, ion beam etching, and ion beam deposition. In negative-ion implantation the charge-up of implanted material surfaces is greatly reduced, and thus ion implantation without target charging is possible. The etching rate due to fluorine-negative ion is mainly determined by its kinetic energy. Pure diamondlike carbon films with high $sp^3$ structure have been prepared by $C^-$ and $C_2^-$ ion beam deposition, and CN films by $CN^-$ ion beam deposition. Negative ions provide an excellent tool for materials processing applications. © *2000 American Institute of Physics.* [S0034-6748(00)51302-1]

## I. INTRODUCTION

Ion beam applications in materials science such as ion implantation, ion beam etching, and ion beam deposition are currently performed by using positive ions. The reason is simple: it was believed that heavy negative ions could not be effectively produced and that there was no difference between negative and positive ions in ion–material interactions.

It has been clarified that heavy negative ions can be effectively produced by surface effect processes, i.e., sputtered particle emission from a cesiated target surface. For optimum surface conditions, the negative-ion production efficiency of sputtered particles is relatively high, i.e., from a few percent to more than 20%.[1] This efficiency is much higher than the ionization efficiency of sputtered particles in sputter-type positive-ion sources. Thus, submilliampere and milliampere heavy-negative-ion beams have been produced by sputter-type negative-ion sources,[2–4] and high current dc mode ion beams have also been obtained from plasma-sputter-type negative-ion sources.[5–7] A dc mode ion beam is essential for ion-beam materials processing.

Negative ions have different features from positive ions,[8] the charge polarities are opposite; as for the internal potential energy, the absolute value of the electron affinity (about 1 eV) for negative ions is much smaller than the ionization potential (about 10 eV). When an ion is neutralized, the electron affinity energy is absorbed from the surroundings for the case of a negative ion, while the the ionization potential energy is ejected to the surroundings. The difference between these features leads to the difference between negative-ion- and positive-ion-material interactions.

Although the surface charging of insulated materials during positive-ion implantation can be quite large and troublesome, surface charging during negative-ion implantation is extremely low and in fact negligible.[7–10] This is caused by the difference of their charge polarities. Chargingless ion implantation will be performed when negative ions are used for implantation. Negative-ion implantation into large scale integrated (LSI) chips without damage to gate insulator[11] or into micron-sized particles without particle scattering[12] is possible. In the case of negative-ion implantation into polymers, the cell-adhesion properties of implanted surfaces can be controlled.[13] The formation of micron-sized metal particles by high dose metal-negative-ion implantation into glass materials can enhance their nonlinear optical properties.[14]

Ion beam etching is mainly caused by the ion kinetic energy. Therefore, there is no large difference between the etching rates by negative and positive ions. It is expected that fluorine-negative ions will etch Si and $SiO_2$ substrates in proportion to the ion momentum.[15]

The kinetic energy of ions used for ion beam deposition is usually as low as several tens to a few hundred eV. Therefore, the internal potential energy of positive ions, i.e., the ionization potential, is comparable with the kinetic energy, or at least is not negligible compared to the kinetic energy. In positive-ion beam deposition, the ionization potential strongly affects the film formation process and sometimes covers the effect of film formation due to the ion kinetic energy. When negative ions are used for ion beam deposition, atomic bonding processes due to the kinetic energy, i.e., kinetic bonding, can be clearly examined because of the small internal potential energy, i.e., electron affinity. Diamondlike carbon (DLC) films with high atomic density and high $sp^3$ structure concentration can prepared by carbon-negative ion beam deposition ($C^-$ and $C_2^-$).[8,16,17] CN films can be formed by CN-negative-ion beam deposition.[18,19]

Thus, new negative-ion beam applications such as negative ion implantation, negative ion etching, and negative ion beam deposition are promising in materials science processing.

[a)]Electronic mail: ishikawa@kuee.kyoto-u.ac.jp

 © 2000 American Institute of Physics

Downloaded 04 Jun 2007 to 130.54.110.22. Redistribution subject to AIP license or copyright, see http://rsi.aip.org/rsi/copyright.jsp

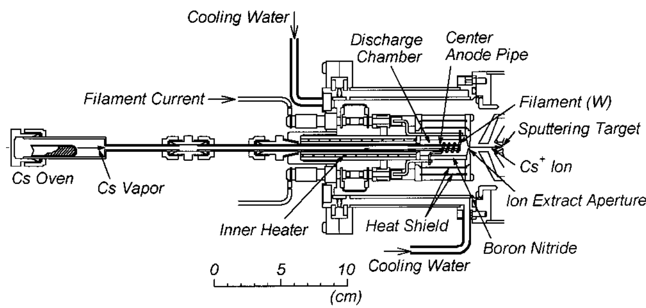


FIG. 1. Neutral- and ionized-alkaline–metal-bombardment-type heavy-negative-ion source (NIABNIS).

TABLE I. Negative ion currents obtained from rf plasma sputter-type heavy-negative-ion source.

| Negative ion | $Cu^-$ | $C^-$ | $C_2^-$ | $Si^-$ | $B_2^-$ | $P^-$ | $O^-$ | $F^-$ | $CN^-$ |
|---|---|---|---|---|---|---|---|---|---|
| Maximum current (mA) | 12.1 | 1.6 | 2.3 | 3.8 | 1.0 | 0.92 | 4.7 | 4.5 | 0.88 |
| Material to be ionized | OFHC | graphite | | poly-Si | sintered $LaBa_8$ | poly-GaAs | $O_2$ gas | $SF_6$ gas | graphite $+N_2$ gas |

## II. SPUTTER-TYPE NEGATIVE-ION SOURCES

We have developed two kinds of sputter-type negative-ion sources: a neutral- and ionized-alkaline–metal-bombardment-type heavy-negative-ion source (NIABNIS),[2] and a rf plasma-sputter-type heavy negative-ion source[5–7] for materials science applications. In the NIABNIS, as shown in Fig. 1, cesium ions and neutral particles are extracted from an electron-bombardment-type ion source, and are irradiated onto a cone-shaped sputter target. If the cesium flux is sufficiently supplied to the sputter target surface, then its work function becomes minimum. Thus, the sputtered particles are effectively changed to negative ions. In this ion source, the same extraction voltage as used for cesium positive ions is also used for the extraction of produced negative ions, which is usually 10–20 kV. From this type of ion source no gas particles are emitted; therefore, it is suited for ion beam deposition application where high vacuum conditions are often required. When nitrogen gas is introduced into a cesium ion source with a graphite sputter target, CN negative ions can be produced.[19] Another version of NIABNIS which has a microwave ion source as a cesium ion and neutral particle source has also been developed to obtain relatively high current negative ions.[17]

In order to obtain milliampere heavy negative ions, an rf plasma sputter-type heavy-negative-ion source as shown in Fig. 2 was developed.[5–7] In this ion source, xenon or argon gas was effectively ionized by an rf (13.56 MHz) discharge at a relatively low gas pressure. A sputter target was negatively biased by several hundred volts, then plenty of xenon or argon ions bombarded on the sputter target surface. When a sufficient neutral cesium flux was supplied to the sputter target surface to make the work function minimum, an efficient negative-ion-production process took place, and milliampere-class negative-ion beams were generated. In order to prevent the negative ions from being destroyed during transport in the plasma region due to electron detachment collisions, a very low gas pressure of $10^{-4}-10^{-5}$ Torr in the plasma generation region was essential. A crossed magnetic field was used to suppress electron emission from the ion source. Under normal operation, a target which consisted of the material to be ionized was used: copper target for $Cu^-$ ions, graphite target for $C^-$ and $C_2^-$ ions, polysilicon target for $Si^-$ ions, sintered $LaB_6$ target for $B_2^-$ ions, poly-GaP target for $P^-$ ions, etc. When gas was fed into the plasma region, negative ions of the gas were produced: $O_2$ gas feed for $O^-$ ions, and $SF_6$ gas feed for $F^-$ ions.[20,21] In special cases, negative ions of compound materials which consisted of target and fed gas materials could be produced: a graphite target and $N_2$ gas feed for $CN^-$ ions.[19] Extracted currents from the rf plasma sputter-type negative-ion source are indicated in Table I. A small version of rf plasma sputter-type negative-ion source was also developed for a negative-ion implanter as shown in Fig. 3.[7]

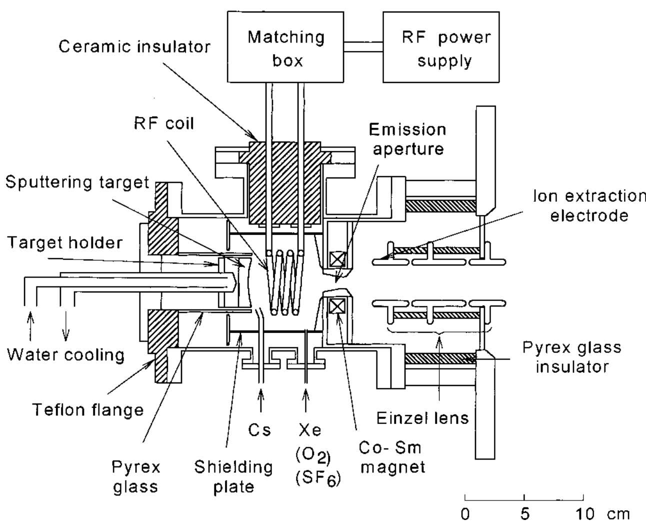


FIG. 2. rf plasma sputter-type heavy-negative-ion source.

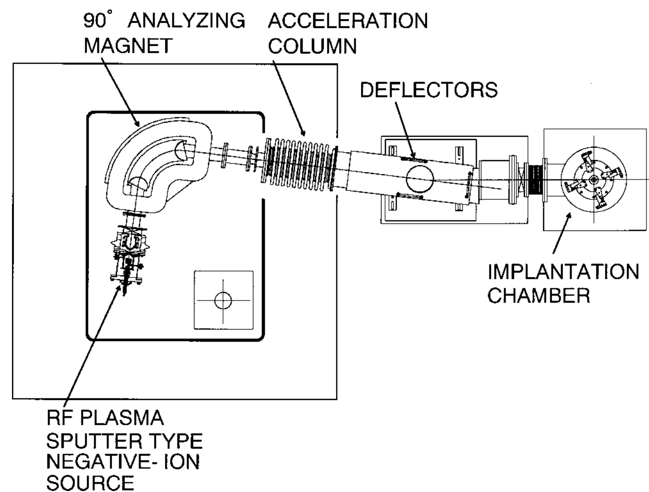


FIG. 3. Negative-ion implanter.

Downloaded 04 Jun 2007 to 130.54.110.22. Redistribution subject to AIP license or copyright, see http://rsi.aip.org/rsi/copyright.jsp

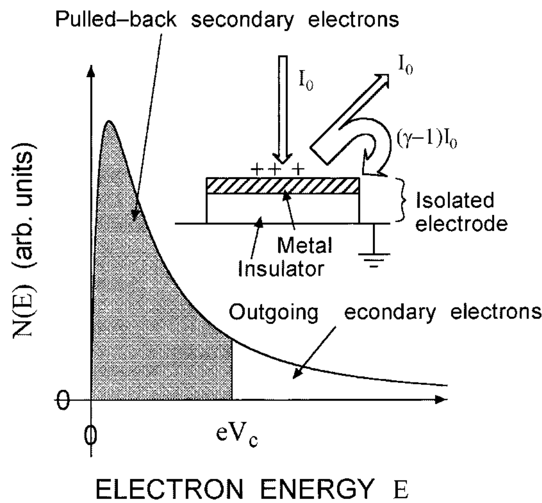


FIG. 4. Schematic diagram illustrating the charge equilibrium of an isolated electrode during negative-ion implantation.

## III. NEGATIVE-ION IMPLANTATION

A negative ion has an electron which is easily released during a collision. Therefore, the secondary electron emission yield due to the bombardment of negative ions is larger by about 1 than that due to the bombardment of positive ions.[22,23] This means that the charging voltage of an insulated material due to negative-ion irradiation is greatly reduced, because the incoming negative charge of the negative ion is easily balanced by the outgoing negative charge of the secondary electron with relatively high energy,[7–11] as shown in Fig. 4. The charging voltage $V_c$ is determined by the following equation:

$$\gamma \int_{eV_c}^{E_{\max}} N(E)\, dE = 1, \tag{1}$$

where $\gamma$ is the secondary electron emission yield, $N(E)$ is the energy distribution function of secondary electrons, and $E_{\max}$ is the maximum energy of secondary electrons. The charging voltage of insulated conductive materials due to negative-ion irradiation is usually positive by several volts, and is 2–4 orders of magnitude lower than that due to positive-ion irradiation. The charging voltage of insulators due to negative-ion irradiation is also very low, i.e., negative by several volts, because an electric double layer is generated on the surface.[24,25] Since the charging voltage of insulated materials due to negative-ion irradiation is between plus–minus several volts, essentially charging-free negative-ion implantation is possible.

### A. Implantation into LSI chips with thin gate oxide

For the case of positive-ion implantation, an electron shower or a plasma neutralizer is used to reduce the charging voltage of the gate electrode during implantation. However, the breakdown voltage of the gate oxide for ultralarge scale integrated (ULSI) circuits will become lower and lower year by year. Thus, utilization of a charge neutralizer will face difficulty. When the negative-ion implantation technique is adapted for LSI fabrication processing, the charging voltage of the gate electrode during implantation is much less than the breakdown voltage without charge neutralizer, and so an implanter with a very simple end station would be possible.

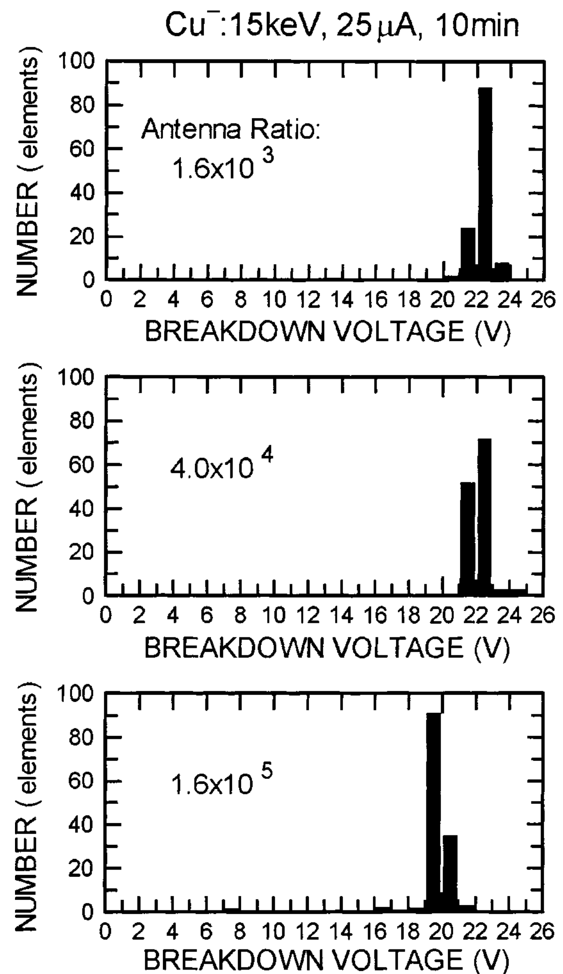


FIG. 5. Breakdown voltage measurement of TEG devices.

For the estimation of ULSI yield rates due to negative-ion implantation, yield rates of a test element group (TEG) device with negative-ion implantation were measured.[10] The TEG device consisted of 130 metal–oxide–semiconductor (MOS) capacitor elements, each of which had a charge-collecting antenna electrode of polysilicon (2×2 mm) and a gate oxide film with a thickness of 20 nm (capacitor region). Three MOS capacitor areas [5×5 $\mu$m (antenna ratio: $1.6\times10^5$), 10×10 $\mu$m (antenna ratio: $4\times10^4$) and 50×50 $\mu$m (antenna ratio: $1.6\times10^3$)] were used. A copper negative-ion beam with an energy of 15 keV and a current of 25 $\mu$A was implanted with a dose of $10^{15}$ ions/cm$^2$. For the case of the devices with an antenna ratio of $1.6\times10^5$, the total charge implanted into the antenna was calculated to be 9.6 C/cm$^2$.

Figure 5 shows the results of breakdown voltage measurements for the TEG device. All devices with antenna ratios of $1.6\times10^3$ and $4\times10^4$ indicated no damage below an applied voltage of 18 V, and 97.7% of the devices with an antenna ratio of $1.6\times10^5$ showed no damage. These results show almost no damage would be expected in ULSI fabrication processes with negative-ion implantation, although most MOS devices with a gate oxide film thickness of 20 nm suffer serious damage under positive-ion implantation with an implanted charge of 10 C/cm$^2$.

Downloaded 04 Jun 2007 to 130.54.110.22. Redistribution subject to AIP license or copyright, see http://rsi.aip.org/rsi/copyright.jsp

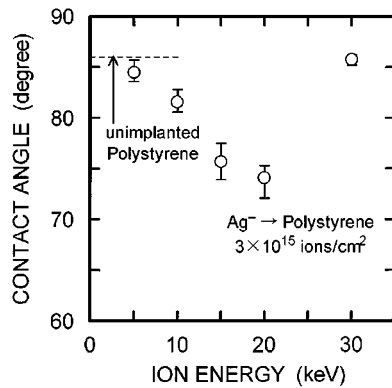


FIG. 6. Contact angle of Ag negative-ion-implanted polystyrene as a function of ion energy, for a constant ion dose of $3\times10^{15}$ ions $cm^{-2}$.

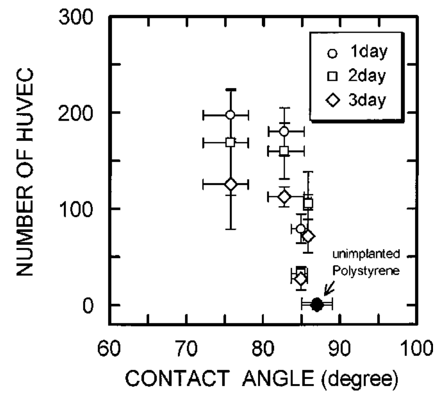


FIG. 7. Change of the number of HUVEC attached to Ag negative ion-implanted polystyrene surfaces with various doses after culture for 1, 2 and 3 d as a function of the contact angle.

## B. Implantation into powder particles

Ion implantation into micron-sized powders such as ceramic and polymer particles is greatly needed for applications in the medical and catalytic fields. When these powder particles are implanted with positive ions, they are scattered by the Coulomb repulsion force due to their strong surface charging, and then implantation to sufficient dose is very difficult.

The critical surface charging voltage of powder particles for scattering depends on the particle diameter, and the minimum value has been measured to be 1 kV.[11,12,26] During negative-ion implantation the surface charging voltage is only several volts, and so is always below the critical value. Therefore, it is expected that no powder particle scattering takes place during negative-ion implantation. When carbon and copper negative-ion beams with energies of 20–40 keV were irradiated with doses of $10^{15}-10^{16}/cm^2$ into various powders (silica and glass beads), no scattering was observed.[12] Therefore, negative-ion beam processing is suited for implantation into powder particles.

## C. Implantation into polymers for cell adhesion

The contact angle of polymers strongly affects cell-adhesion properties. The contact angle of polymers can be controlled by ion implantation, and thus the cell-adhesion properties can be improved within a selectively implanted area.[13,27,28] Since polymers are insulating and a precise implantation energy is essential to cell-adhesion control, charging-less negative-ion implantation is preferable.

Figure 6 shows the contact angle for polystyrene surfaces which were implanted by silver negative ions with a dose of $3.0\times10^{15}$ ions $cm^{-2}$, as a function of the ion energy.[13] The contact angle significantly decreased from 86° to 73° with the increase in ion energy from 5 to 20 keV. Figure 7 shows the number of human umbilical vascular endothelial cells (HUVEC) that attached to the polystyrene surface after culture periods of 1,2, and 3 d as a function of the contact angle. The threshold contact angle was found to be around 85°, below which the surface exhibited good cell-adhesion properties.[13] Thus, the HUVEC adhesion area can be limited to the negative-ion implantation region.

## D. Implantation into glass for nonlinear optical characteristics

When a metal ion such as copper was implanted into glass with a high dose of around $10^{17}$ ions/$cm^{-2}$, ultrafine grains of metals were formed, enhancing the nonlinear optical characteristics of third order.[14] For such a high dose implantation into insulators, charging-less negative-ion implantation is preferable.

## IV. NEGATIVE-ION BEAM ETCHING

Recently much attention has been paid to negative-ion beam etching because of the possibility of charging-less etching, or a combination of positive- and negative-ion-beam etching for charge neutrality. However, no experiment on etching rate due to negative ions has been reported. From the rf plasma sputter-type negative-ion source, milliamperes of fluorine negative ions can be extracted,[20,21] and then measurement of the etching rate due to fluorine negative ions is possible.

Figure 8 shows the etching rate of Si and $SiO_2$ due to fluorine-negative ions as a function of the square root of the ion energy.[15] The etching rate was normalized assuming irradiation with a current density of 1 $mA/cm^2$. The etching rate was proportional to the square root of the ion energy, which means that the sputtering was mainly due to energy transfer by kinetic collisions. Therefore, it is expected that the etching rate due to negative ions would not be much

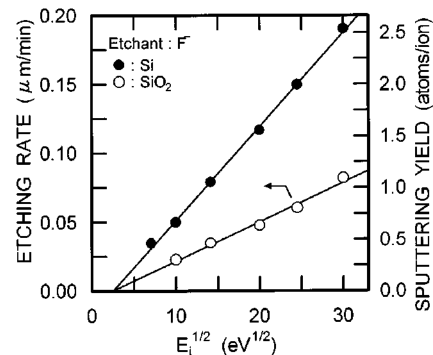


FIG. 8. Etching rate of Si and $SiO_2$ due to fluorine negative ions as a function of square root of the ion energy.

Downloaded 04 Jun 2007 to 130.54.110.22. Redistribution subject to AIP license or copyright, see http://rsi.aip.org/rsi/copyright.jsp

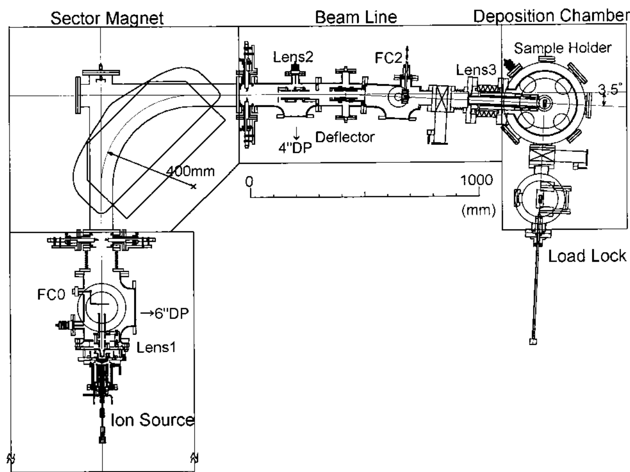


FIG. 9. Negative-ion-beam depositor.

different from that due to positive ions, and the difference appears in their charge polarity and charging properties.

## V. NEGATIVE-ION BEAM DEPOSITION

For negative-ion beam deposition a depositor as shown in Fig. 9 was developed.[29] Since pure films were desired, the NIABNIS, which emitted no gas particles, was used in the depositor. The background gas pressure of the deposition chamber was $2\times10^{-9}$ Torr. The negative current was 20–30 $\mu$A for $C^-$ deposition, 10–15 $\mu$A for $C_2^-$ deposition, and 5–10 $\mu$A for $CN^-$ deposition. The energy range of the ion beam used for the deposition was between 20 and 1000 eV. The energy spread of the negative ion beams was about 10 eV; for example, 6.8 eV for a $Ag^-$ ion beam and 13.5 eV for a $C^-$ ion beam.[30] The initial energy of negative ions when sputtered was as low as a few eV; for example, 1.6 eV for $Ag^-$ ions and 5.0 eV for $C^-$ ions. Thus, by using negative ions, ion beam deposition with an exact deposition energy can be performed.

### A. DLC films

Figure 10 shows the $sp^3$ fraction as a function of the incident ion energy for films formed by $C^-$ and $C_2^-$ ion-beam deposition on silicon substrates. The incident ion energy

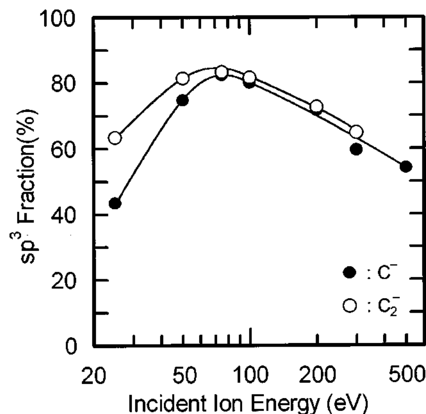


FIG. 10. The $sp^3$ fraction as a function of incident ion energy for films formed by $C^-$ and $C_2^-$ ion beam deposition.

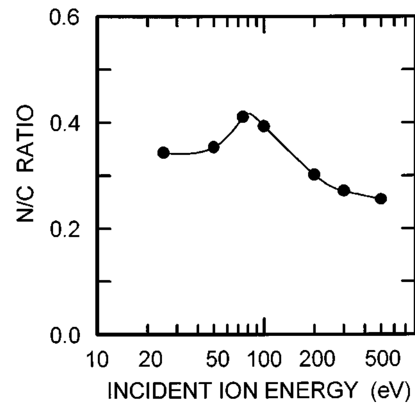


FIG. 11. The N/C ratio as a function of incident ion energy for films formed by $CN^-$ ion beam deposition.

means kinetic energy per atom in this Fig. 10. The $sp^3$ fraction strongly depended on the negative-ion kinetic energy, having a peak at an energy of around 50–100 eV. This means that the $sp^3$ bonding due to kinetic energy, i.e., kinetic bonding which enhances metastable crystal structure, would proceed at a kinetic energy of 50–100 eV atom.

### B. CN films

Figure 11 shows the N/C ratio as a function of the incident energy of $CN^-$ ions for films formed by $CN^-$ ion-beam deposition on silicon substrates. The N/C ratio was evaluated from XPS measurements of the film surface. The film with a high N/C ratio was prepared at a kinetic energy of around 100 eV, at which energy metastable structures would be selectively formed by kinetic bonding.


[1] J. Ishikawa, H. Tsuji, Y. Gotoh, and Azegami, AIP Conf. Proc. **287**, 66 (1992).
[2] J. Ishikawa, Y. Takeiri, H. Tsuji, T. Taya, and T. Takagi, Nucl. Instrum. Methods Phys. Res. B **232**, 186 (1984).
[3] G. D. Alton, Y. Mori, A. Takagi, A. Ueno, and S. Fukumoto, Rev. Sci. Instrum. **61**, 372 (1990).
[4] Y. Mori, Rev. Sci. Instrum. **63**, 2357 (1992).
[5] J. Ishikawa, H. Tsuji, Y. Okada, M. Shinoda, and Y. Gotoh, Vacuum **44**, 203 (1993).
[6] H. Tsuji, J. Ishikawa, Y. Okayama, Y. Toyota, and Y. Gotoh, *Proceedings of Ion Implantation Technology-94* (Elsevier, Amsterdam, 1995), p. 495.
[7] J. Ishikawa, H. Tsuji, Y. Toyota, Y. Gotoh, K. Matsuda, M. Tanjo, and S. Sakai, Nucl. Instrum. Methods Phys. Res. B **96**, 7 (1995).
[8] J. Ishikawa, Surf. Coat. Technol. **65**, 64 (1994).
[9] J. Ishikawa, Mater. Res. Soc. Symp. Proc. **354**, 99 (1995).
[10] J. Ishikawa, Rev. Sci. Instrum. **65**, 1290 (1994).
[11] J. Ishikawa, *Application of Accelerators in Research and Industry* (AIP, New York, 1997), p. 915.
[12] J. Ishikawa, H. Tsuji, M. Mimura, S. Ikemura, and Y. Gotoh, Surf. Coat. Technol. **103/104**, 173 (1998).
[13] H. Tsuji, H. Satoh, S. Ikeda, N. Ikemoto, Y. Gotoh, and J. Ishikawa, Surf. Coat. Technol. **103/104**, 124 (1998).
[14] N. Kishimoto, V. T. Gritsyna, K. Kono, H. Amekura, and T. Saito, Mater. Res. Soc. Symp. Proc. **438**, 435 (1997).
[15] J. Ishikawa, H. Tsuji, K. Shibutani, Y. Ikai, and Y. Gotoh, Presented at the 12th International Conference on Ion Implantation Technology, Kyoto, Japan, June 22–26, 1998, P1-118.
[16] J. Ishikawa, *New Horizons for Materials* (Techna, Faenza, 1995), p. 399.
[17] J. Ishikawa, Y. Takeiri, and T. Tagaki, Rev. Sci. Instrum. **57**, 1512 (1993).
[18] H. Tsuji, J. Ishikawa, T. Tomita, T. Yoshihara, and T. Gotoh, Rev. Sci. Instrum. **69**, 884 (1998).
[19] H. Tsuji, T. Yoshihara, S. Nakamura, Y. Gotoh, and J. Ishikawa, Pre-


Downloaded 04 Jun 2007 to 130.54.110.22. Redistribution subject to AIP license or copyright, see http://rsi.aip.org/rsi/copyright.jsp

sented at the 11th International Conference on Ion Beam Modification of Materials, Amsterdam, 1998, pp. 20–11.
[20] H. Tsuji, J. Ishikawa, T. Tomita, and Y. Gotoh, Rev. Sci. Instrum. **67**, 1012 (1996).
[21] H. Tsuji, J. Ishikawa, T. Tomita, and Y. Gotoh, Proc. IEEE **8182**, 334 (1997).
[22] Y. Toyota, H. Tsuji, Y. Gotoh, and J. Ishikawa, Jpn. J. Appl. Phys., Part 1 **34**, 6487 (1995).
[23] J. Ishikawa, H. Tsuji, S. Ikeda, and Y. Gotoh, Nucl. Instrum. Methods Phys. Res. B **127/128**, 282 (1997).
[24] H. Tsuji, J. Ishikawa, S. Ikeda, and Y. Gotoh, Nucl. Instrum. Methods Phys. Res. B **127/128**, 278 (1997).
[25] H. Tsuji, Y. Gotoh, and J. Ishikawa, Nucl. Instrum. Methods Phys. Res. B **141**, 645 (1998).
[26] J. Ishikawa, H. Tsuji, and Y. Gotoh, Proc. IEEE **8182**, 249 (1997).
[27] H. Tsuji, H. Satoh, S. Ikeda, Y. Gotoh, and J. Ishikawa, Nucl. Instrum. Methods Phys. Res. B **141**, 197 (1998).
[28] H. Sato, H. Tsuji, S. Ikeda, N. Ikemoto, J. Ishikawa, and S. Nishimoto, J. Biomed. Mater. Res. **44**, 22 (1999).
[29] J. Ishikawa, Proceedings of the 7th International Symposium on Advanced Nuclear Energy Research, Takasaki, Japan, 1997, JAERI-Conf. 97-003, p. 149.
[30] J. Ishikawa, H. Tsuji, T. Takatori, and Y. Gotoh, AIP Conf. Proc. **380**, 241 (1996).

**Downloaded 04 Jun 2007 to 130.54.110.22. Redistribution subject to AIP license or copyright, see http://rsi.aip.org/rsi/copyright.jsp**